AIAA 2002–5598

Design of a Low-Boom Supersonic Business Jet Using Cokriging Approximation Models

Hyoung-Seog Chung and Juan J. Alonso
Stanford University, Stanford, CA 94305

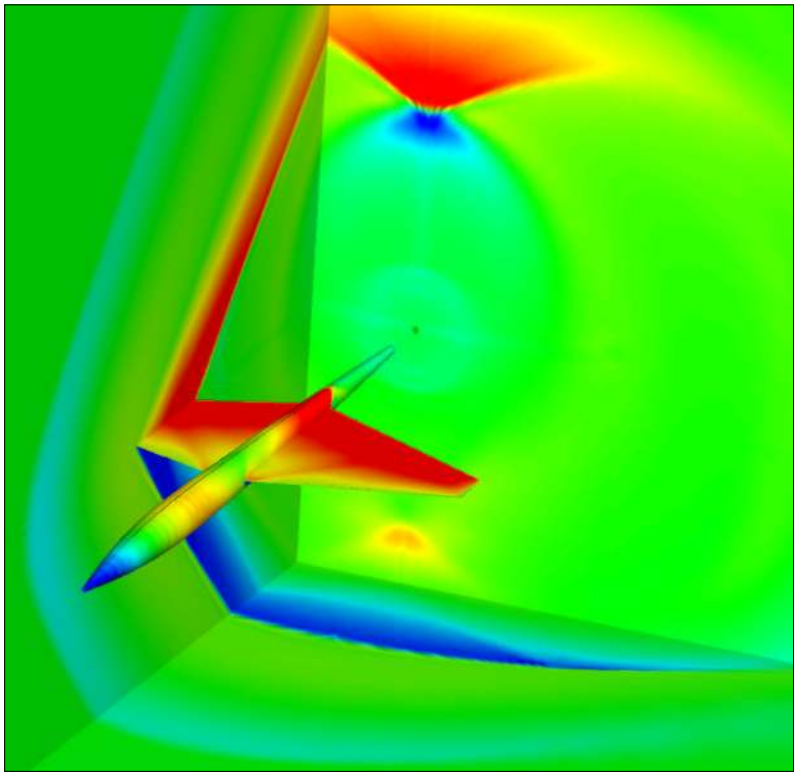

9th AIAA/ISSMO Symposium on Multidisciplinary Analysis and Optimization
September 4–6, 2002/Atlanta, Georgia

AIAA 2002–5598

Design of a Low-Boom Supersonic Business Jet Using Cokriging Approximation Models

Hyoung-Seog Chung* and Juan J. Alonso†
Stanford University, Stanford, CA 94305

In this paper we study the ability of the Cokriging method to represent functions with multiple local minima and sharp discontinuities for use in the multidimensional design of a low-boom supersonic business jet wing-body-canard configuration. Cokriging approximation models are an extension of the original Kriging method which incorporate secondary information such as the values of the gradients of the function being approximated. Provided that gradient information is available through inexpensive algorithms such as the adjoint method, this approach greatly improves on the accuracy and efficiency of the original Kriging method for high-dimensional design problems. In order to construct Cokriging approximation models, an automated Euler and Navier-Stokes based method, QSP107, has been developed to provide accurate performance and boom data with very rapid turnaround. The resulting approximations are used with a simple gradient-based optimizer to improve a multi-objective cost function with large variations in the design space. Results of sample two-dimensional test problems, together with a 15-dimensional test case are presented and discussed. The Cokriging method is a viable alternative to quadratic response surface methods for preliminary design using a moderate number of design variables, particularly when the cost function being optimized is very nonlinear.

Nomenclature

β	constant underlying global portion of Kriging model
C_D	drag coefficient
$\boldsymbol{f}$	constant vector used in Kriging model
$\boldsymbol{f}_c$	constant vector used in Cokriging model
k	number of design variables
n_s	number of sample points
$\boldsymbol{r}$	vector of correlation values for Kriging model
$\boldsymbol{r}_c$	vector of correlation values for Cokriging model
$R(.)$	correlation function for Kriging model
$\boldsymbol{R}$	correlation matrix for Kriging model
$\boldsymbol{R}_c$	correlation matrix for Cokriging model
x	scalar component of $\boldsymbol{x}$
$\boldsymbol{x}^p$	vector denoting the p^{th} location in the design space
$y(.)$	unknown function
$\hat{y}(.)$	estimated model of y(.)
$\boldsymbol{\theta}$	vector of correlation parameters for Kriging model
$\hat{\sigma}^2$	estimated sample variance

*Doctoral Candidate, AIAA Member
†Assistant Professor, Department of Aeronautics and Astronautics , AIAA Member

1. Introduction

THE optimization of aerospace systems is an iterative process that requires computational models embodied in complex and expensive analysis software. This paradigm is well exemplified by the field of Multidisciplinary Design Optimization (MDO) which attempts to exploit the synergism of mutually interacting disciplines in order to improve the performance of a given design, while increasing the level of confidence that the designer places on the outcome of the design itself. MDO methods, particularly those based on high-fidelity analyses, greatly increase the computational burden and complexity of the design process.[1–4] For this reason, high-fidelity analysis software typically used in single discipline designs may not be suitable for direct use in MDO.[2,5] Faced with these problems, the alternative of using approximation models of the actual analysis software has received increased attention in recent years. A second advantage of using approximation models during the optimization process is that, since their evaluation is inexpensive, they can be used with optimization algorithms which do not rely on the computation of sensitivity derivatives.

One of the most common methods for building an approximate model is the Response Surface Method (RSM) in which a polynomial function of varying order

(usually a quadratic function) is fitted to a number of sample data points using least squares regression. This method has achieved popularity since it provides an explicit functional representation of the sampled data, and is both computationally inexpensive to run and easy to use. However, response surface models have several key limitations: their accuracy is only guaranteed within a small trust region, and, by design, they are unable to predict multiple extrema. In addition, these methods were originally developed to model data resulting from physical experiments which had a random error distribution. Since the nature of computer experiments is such that random errors are not present (a bias is much more common), the use of these methods for modeling deterministic data has resulted in serious debate within the statistical community.[6] In order to overcome these problems, Sacks, et al.[7] proposed an interpolation modeling technique, known as the Kriging method, developed in the fields of spatial statistics and geostatistics, in order to approximate the results of deterministic computer analyses. The Kriging method is different from the RSM since the interpolation of the sampled data is carried out using a maximum likelihood estimation procedure,[8] which allows for the capturing of multiple local extrema. The Kriging method, however, is more expensive to evaluate than a traditional quadratic response surface, although the cost of evaluation is still orders of magnitude smaller than the costly CFD simulations that it is attempting to approximate. In addition, it does not provide an explicit equation for the approximation. Finally, but most importantly, just as any approximation model, the accuracy of a Kriging model depends greatly on the number of sample data points used and their locations in multidimensional space. In order to fully exploit the advantages of Kriging models, a large number of sample data points must be distributed within the design space. This sampling process can be very costly and even impractical in high-dimensional design optimization using high-fidelity methods.

The Cokriging method is an extension of the Kriging method that incorporates gradient information in addition to primary function values when generating approximation models. Provided that gradient information is available through inexpensive algorithms such as the adjoint approach, the Cokriging method can use this relatively cheap gradient information in lieu of the computationally expensive functional evaluations (CFD analyses in our case). This was the objective that we were trying to accomplish when the Cokriging method was first used in aerospace applications. Using this approach one can approximate the original function with a much smaller number of samples, without significantly sacrificing the accuracy of the approximation. The gradient information at each sample point provides a wealth of information, since it is calculated with respect to all the design variables in the problem. This information can be directly built into the Cokriging formulation as we had described in [9] in what we called the *Direct Cokriging* method. Alternatively, the gradient information can be included in an *augmented* Kriging model by adding new points to the sample database that are obtained using a linear Taylor series expansion about the points at which the gradients were computed. This procedure was also followed by Liu and Batill[10] who called it *Database Augmentation*. In their work, an assessment of the distances used to add new sample points was made, together with a study of three methods to obtain the values of the Kriging approximation parameters by minimizing different norms of the approximation error. In our previous work, we had only found small differences between the Direct Cokriging and Database Augmentation approaches for the chosen sample functions. Our intent is to use these approximations models for highly nonlinear cost functions which may even include discontinuities. Since the quality of the approximation is to a certain extent dependent on both the number of sample data points and their locations, both alternatives must be considered as potential candidates.

In this paper, our intention is to further explore the suitability of Cokriging models for multidimensional design cases where the cost functions being approximated can have both multiple local minima and discontinuities. For this purpose, we have chosen the aerodynamic shape design of a low-boom supersonic business jet. The purpose of this multi-objective design optimization problem is to reduce the sonic boom signature at the ground by modifying the aircraft configuration parameters while preserving or improving aerodynamic performance. In order to make sure that a number of local minima are present in the design, we have setup a very large design space which allows for significant variations in the configuration.All designs and approximations are based on the solution of the Euler equations of the fluid on meshes that are properly resolved (3×10^6 nodes and above) for the computation of near-field pressures that can be used to compute ground boom distributions. A nonlinear integrated boom analysis tool, QSP107, which incorporates an automated mesh generation routine, a three-dimensional Euler flow solver, and a boom propagation procedure that is based on geometric acoustics and nonlinear wave propagation has been developed and is used for sonic boom prediction. Section 2 presents an overview of the derivation of the Kriging and Cokriging methods (in both of their forms). Section 3 describes the 15-dimensional test case that we use in this work, together with two different 2-dimensional simplifications that will be used to visually examine the nature of the functions being approximated and the suitability of Kriging and Cokriging methods for these types of functions. Section 4 describes the fast turnaround non-

linear analysis environment that we have developed to provide sample data points and gradients for the approximations. Finally, Section 5 presents the results of our 2- and 15-dimensional test cases with several comparisons between Kriging and Cokriging approximations.

2. Overview of Kriging Method

2.1 Original Kriging Method

The Kriging technique uses a two component model that can be expressed mathematically as

$$y(\boldsymbol{x}) = f(\boldsymbol{x}) + Z(\boldsymbol{x}), \tag{1}$$

where $f(\boldsymbol{x})$ represents a global model and $Z(\boldsymbol{x})$ is the realization of a stationary Gaussian random function that creates a localized deviation from the global model.[11] If $f(x)$ is taken to be an underlying constant,[8] β , Equation (1) becomes

$$y(\boldsymbol{x}) = \beta + Z(\boldsymbol{x}), \tag{2}$$

which is used in this paper. The estimated model of Equation (2) is given as

$$\hat{y} = \hat{\beta} + \boldsymbol{r}^T(\boldsymbol{x})\boldsymbol{R}^{-1}(\boldsymbol{y} - \boldsymbol{f}\hat{\beta}), \tag{3}$$

where $\boldsymbol{y}$ is the column vector of response data and $\boldsymbol{f}$ is a column vector of length n_s which is filled with ones. $\boldsymbol{R}$ in Equation (3) is the correlation matrix which can be obtained by computing $R(\boldsymbol{x}^i, \boldsymbol{x}^j)$, the correlation function between any two sampled data points. This correlation function is specified by the user. In this work, the authors use a Gaussian exponential correlation function of the form provided by Giunta, et al.[6]

$$R(\boldsymbol{x}^i, \boldsymbol{x}^j) = \exp\left[-\sum_{k=1}^{n} \theta_k |\boldsymbol{x}_k^i - \boldsymbol{x}_k^j|^2\right]. \tag{4}$$

The correlation vector between $\boldsymbol{x}$ and the sampled data points is expressed as

$$\boldsymbol{r}^T(\boldsymbol{x}) = [R(\boldsymbol{x}, \boldsymbol{x}^1), R(\boldsymbol{x}, \boldsymbol{x}^2), ..., R(\boldsymbol{x}, \boldsymbol{x}^n)]^T. \tag{5}$$

The value for $\hat{\beta}$ is estimated using the generalized least squares method as

$$\hat{\beta} = (\boldsymbol{f}^T\boldsymbol{R}^{-1}\boldsymbol{f})^{-1}\boldsymbol{f}^T\boldsymbol{R}^{-1}\boldsymbol{y}. \tag{6}$$

Since $\boldsymbol{R}$ is a function of the unknown variable $\boldsymbol{\theta}$, $\hat{\beta}$ is also a function of $\boldsymbol{\theta}$. Once $\boldsymbol{\theta}$ is obtained, Equation (3) is completely defined. The value of $\boldsymbol{\theta}$ is obtained by maximizing the following function over the interval $\boldsymbol{\theta} > \boldsymbol{0}$

$$-\frac{[n_s \ln(\hat{\sigma}^2) + \ln|\boldsymbol{R}|]}{2}, \tag{7}$$

where

$$\hat{\sigma}^2 = \frac{(\boldsymbol{y} - \boldsymbol{f}\hat{\beta})^T\boldsymbol{R}^{-1}(\boldsymbol{y} - \boldsymbol{f}\hat{\beta})}{n_s}. \tag{8}$$

2.2 Direct Cokriging Method

In order to construct a Kriging approximation the only data required are the function values at a number of pre-specified sample locations. For many computational methods, secondary information such as gradient values may be available as a result of the analysis procedure. Alternatively, the gradient vector can be computed with very little additional cost, as is the case in the adjoint method.[3] Gradient information is usually well cross-correlated with the function values and thus contains useful additional information. The Cokriging method can approximate the unknown primary function of interest more effectively by using these secondary function values.[12] This section briefly describes the theory behind Cokriging approximations.

For the original Kriging method, the covariance matrix of $Z(\boldsymbol{x})$ is defined as

$$\text{Cov}\left[y(\boldsymbol{x}^i), y(\boldsymbol{x}^j)\right] = \sigma^2\boldsymbol{R}\left[R\left(\boldsymbol{x}^i, \boldsymbol{x}^j\right)\right], \tag{9}$$

where $\boldsymbol{R}$ is the correlation matrix and $R\left(\boldsymbol{x}^i, \boldsymbol{x}^j\right)$ is the correlation function given by Equation (4). Since the correlation matrix $\boldsymbol{R}_c$ and the correlation vector $\boldsymbol{r}_c$ for the Cokriging method are evaluated using not only function values at the sample points, but also with their gradient, the covariance can be modified as follows

$$\begin{aligned}
\text{Cov}\left[y(\boldsymbol{x}^i), y(\boldsymbol{x}^j)\right] &= \sigma^2\boldsymbol{R}\left[R\left(\boldsymbol{x}^i, \boldsymbol{x}^j\right)\right], &(10)\\
\text{Cov}\left[y(\boldsymbol{x}^i), \frac{\partial y(\boldsymbol{x}^j)}{\partial x_k}\right] &= \sigma^2\frac{\partial R(\boldsymbol{x}^i, \boldsymbol{x}^j)}{\partial x_k}, &(11)\\
\text{Cov}\left[\frac{\partial y(\boldsymbol{x}^i)}{\partial x_k}, y(\boldsymbol{x}^j)\right] &= -\sigma^2\frac{\partial R(\boldsymbol{x}^i, \boldsymbol{x}^j)}{\partial x_k}, &(12)\\
\text{Cov}\left[\frac{\partial y(\boldsymbol{x}^i)}{\partial x_k}, \frac{\partial y(\boldsymbol{x}^j)}{\partial x_l}\right] &= -\sigma^2\frac{\partial R(\boldsymbol{x}^i, \boldsymbol{x}^j)}{\partial x_k \partial x_l}. &(13)
\end{aligned}$$

Accordingly, the Cokriging model can be obtained by modifying Equation (3) to yield

$$\hat{y_c} = \hat{\beta_c} + \boldsymbol{r}_c^T(\boldsymbol{x})\boldsymbol{R}_c^{-1}(\boldsymbol{y}_c - \boldsymbol{f}_c\hat{\beta_c}), \tag{14}$$

and

$$\hat{\beta_c} = (\boldsymbol{f}_c^T\boldsymbol{R}_c^{-1}\boldsymbol{f}_c)^{-1}\boldsymbol{f}_c^T\boldsymbol{R}_c^{-1}\boldsymbol{y}_c, \tag{15}$$

where

$$\begin{aligned}
\boldsymbol{y}_c &= \left[y(\boldsymbol{x}^1), ..., y(\boldsymbol{x}^{n_s}), \frac{\partial y(\boldsymbol{x}^1)}{\partial \boldsymbol{x}_1}, \frac{\partial y(\boldsymbol{x}^1)}{\partial \boldsymbol{x}_2}, ... \frac{\partial y(\boldsymbol{x}^{n_s})}{\partial \boldsymbol{x}_k}\right],\\
\boldsymbol{f}_c &= [1, 1, ..., 1, 0, 0, ..., 0],
\end{aligned}$$

and $\boldsymbol{f_c}$ contains n_s ones and $n_s \times k$ zeros. The reader is referred to Refs[7, 11, 12] for more details on the development of the Kriging and Cokriging techniques.

2.3 Indirect Cokriging

Another way to include gradient information in the Kriging method is to create additional function values using the gradients available and a first order Taylor series expansion in a close neighborhood of the

sample point. In this approach, the original Kriging formulation can be used with an increased number of sample data values. These additional function values play a similar role to the gradients since they tend to have strong correlations with the original sample points given the close distances to each other. The authors have given this approach the name Indirect Cokriging only to distinguish it from the Cokriging (Direct Cokriging) method which uses the gradient information directly. Both of these approaches are used in the results presented in this paper. Liu et al.[10] refer to the Indirect Cokriging method by the name of Database Augmentation: although different error estimation criteria may be used, both approaches are similar in nature.

3. Test Problem : Low-Boom Supersonic Business Jet (SBJ) Design

The design problem in question involves the ground boom and drag minimization of a supersonic business jet wing-body-canard configuration at a specified lift coefficient, $C_L = 0.8885$, which corresponds to a cruise weight of $100,000$ lbs at a cruise flight altitude of $50,000$ ft. The aircraft geometry and flow conditions were parameterized with a total of 70 potential design variables. Three different test problems will be presented in the Results section. These problems include two two-dimensional test cases used for validation and demonstration and one 15-dimensional case used to establish the feasibility of the method in higher dimensional spaces.

3.1 2-Dimensional Validation Case

For the initial validation test case, two geometric design variables were chosen so that the actual objective function and its Cokriging approximation could be graphically compared and validated. In this case, we selected as design variables the streamwise position of the wing along the surface of the fuselage measured from its nose, and the radius of the fuselage station located halfway between the nose and the tail. This choice of design variables was found to produce a smoothly varying objective function (C_D) with multiple local extrema. This design space was used as a realistic test function for the visualization of Cokriging models.

3.2 2-Dimensional Design Problem

In order to address the ability of Cokriging approximations to effectively deal with objective functions with discontinuities, a 2-dimensional SBJ design problem was set up in which both the coefficient of drag, C_D, and the ground boom overpressure were minimized using successive Cokriging models and a trust region methodology. The ground boom overpressure was evaluated by simply measuring the strength of the first pressure discontinuity in the signature. More elaborate measures of overpressure (dBA, impulse, etc.) could be easily incorporated. The chosen design variables represent the following geometric parameters:

x_1 = fuselage radius at 10% of fuselage length
x_2 = fuselage radius at 20% of fuselage length

Variations in these design variables were used to compute aerodynamic coefficients and ground boom pressure distribution at 5 sample design points chosen by incrementing and decrementing each variable from the baseline value using a straightforward design of experiments approach. Two additional flow solutions were calculated at each sample points to collect finite-difference gradient information along each design variable. The step size was chosen to be 0.1% of the value of the corresponding design variable. In a realistic design environment the gradient information would be obtained using our adjoint approach. Using 5 sample values and 10 gradient components (two at each sample point), indirect Cokriging models for both C_D and ground boom overpressure were generated and used in design optimization. The approximation and optimization procedure was repeated three times for the boom optimization case to graphically demonstrate the feasibility of using Cokriging models for sonic boom minimization.

3.3 15-Dimensional Design Problem

The design problem was extended to a 15 design variable problem to test the procedure in a more realistic design environment. The list of geometric influences of the design variables is given below and in Figure 9:

x_1 = canard wing sweep angle at $c/4$ line
x_2 = canard position along fuselage
x_3 = canard linear twist angle
x_4 = wing sweep angle at $c/4$ line
x_5 = wing aspect ratio
x_6 = wing taper ratio
x_7 = wing dihedral angle
x_8 = wing root thickness-to-chord(TOC) ratio
x_9 = wing tip thickness-to-chord(TOC) ratio
x_{10} = wing tip linear twist angle
x_{11} = fuselage radius at 3% of fuselage length
x_{12} = fuselage radius at 10% of fuselage length
x_{13} = fuselage radius at 20% of fuselage length
x_{14} = fuselage radius at 30% of fuselage length
x_{15} = fuselage radius at 50% of fuselage length

The airfoil sections for the canard and main wing were chosen to be simple biconvex airfoils of varying thickness. The free-stream flow conditions were fixed at $M_\infty = 2.0$ and the coefficient of lift, based on a wing planform area of $1,650$ ft^2, a gross weight of

100,000 lbs and a cruise altitude of 50,000 ft, was fixed at $C_L = 0.08885$. Once each CFD calculation had converged a minimum of 4 orders of magnitude in the average density residual, a near-field pressure distribution was extracted at a distance of 1.2 times the fuselage length below of the body on the symmetry plane. The pressure signature was then provided to the boom propagation code to estimate ground sonic boom characteristics. As in the previous test case, the initial pressure rise at the ground was used as the measure of overpressure.

The C_D and boom overpressure Cokriging models were incorporated into a nonlinear optimization process using MATLAB's *fmincon* to perform design optimizations. All design variables were allowed to span a large design space. These large variations, when not properly constrained, can lead to unrealistic designs. As will be shown in the Results section, this is indeed the case in this test case. However, our intention was for this test case to serve as a demonstration of the capabilities of both our automated CFD system and the Cokriging approximations and not as an actual usable design.

4. Design Tools

In order to develop Kriging and Cokriging approximation models, a large number of CFD computations for different geometries must be carried out automatically. For this purpose, we have developed a nonlinear integrated boom analysis tool, QSP107, that can provide both ground boom and aerodynamic performance information for a small set of configuration variables that are provided in an input file.

4.1 QSP107

A nonlinear integrated boom analysis tool has been developed for sonic boom prediction based on fully nonlinear CFD analyses. This tool couples the multiblock Euler and Navier-Stokes flow solver FLO107-MB[13] to an H-mesh generator adapted from the HFLO4 code of Jameson and Baker,[14] and to the PC Boom software for far-field propagation developed by Wyle Associates.[20] A flowchart of the automated analysis process can be seen in Figure 8.

The procedure starts with a geometry generation module that automatically creates the necessary surface meshes to describe the configuration in question. This geometry module is simply based on a parametric aircraft description with 67 design variables of which a subset (either two or fifteen as discussed earlier) are chosen for our optimization experiments. The H-type mesh, which is generated automatically from the parametric geometry definition, can handle arbitrary wing-fuselage-canard configurations. The grid is then adjusted to have higher resolution in the areas where shock waves and expansions are present below the aircraft, and its grid lines are slanted at the Mach angle to maximize the resolution of the pressure signature at distances of the order of one body length. The user may specify the location of an arbitrary cylindrical surface where the near-field signature is extracted from the multiblock flow solution and provided as an input to a modified version of PC Boom which propagates a full three-dimensional signature along all rays that reach the ground. This allows for the calculation of arbitrary cost functions (not only ground-track initial overpressure) that may involve weighted integration of the complete sonic boom footprint. In this work, however, only the ground track overpressure has been considered. The flow solver combines advanced multigrid procedures and a preconditioned explicit multistage time stepping algorithm which allows full parallelization.

Because of the advanced solution algorithms and parallelization, the integrated tool provides fully nonlinear simulations with very rapid turnaround time. Using typical meshes with over 3×10^6 mesh points we can obtain a complete flow solution and ground signature prediction in under 5 minutes, using 16 processors of a Beowulf cluster made up of 1.2Ghz AMD Athlon processors. In this work, we have used QSP107 repeatedly to generate Kriging and Cokriging approximation models which required 496 of these solutions for each approximation step.

4.2 Optimization Algorithm

Given that both Kriging and Cokriging approximation models can handle cost functions with multiple local minima and discontinuities, the logical choice of optimization algorithm would be one that can perform global searches in a robust fashion. It is our intention to use this kind of methods in the near future, but for the time being we have chosen to use a constrained gradient-based optimizer to perform all computations. The medium-scale optimization algorithm we have used is the *fmincon* algorithm in the optimization toolbox of MATLAB.[21] *fmincon* uses a Sequential Quadratic Programming algorithm. In this method, a Quadratic Programming (QP) subproblem is solved at each major iteration. An estimate of the Hessian of the augmented Lagrangian is updated at each iteration using the BFGS formula. Line searches are used, and the QP subproblem is solved using an active set solution strategy.

In order to avoid getting trapped in a local minimum, for each Cokriging approximation, a number of optimizations are performed starting from randomly chosen initial conditions within the design space, including the baseline point. Although this is no guarantee of having arrived at the global optimum, the minimum of all these optimizations is considered to be the global optimum for the current approximation model. This procedure is repeated as the trust region size is decreased and the Cokriging approximations are

refined.

5. Results

5.1 Graphical Validation of Cokriging Method

Two-dimensional Cokriging models were created for the C_D of the supersonic business jet test problem using sample data obtained from CFD analyses in order to validate and investigate their ability to approximate the results of the original CFD code. The two design parameters of the wing-body configuration chosen as design variables were the wing streamwise location along fuselage and the radius of the fuselage at its mid-point. 400 CFD calculations were performed by varying the design variables to obtain a graphical representation of the actual CFD analyses. The results are shown in Figure 1 (a). The design variables were chosen so as to generate a realistic test function having multiple local extrema to check the ability of Cokriging models to simulate this feature. One important point to note from the Figure is that the actual drag coefficient varies smoothly with respect to the geometric design variables. The selection of Gaussian exponential correlation function for the Kriging method was based on the assumption that the response function to be modeled was very smooth in nature. Thus, Figure 1 (a) provides the validation of the assumption and the rationale for using the Gaussian correlation function in this problem.

A total of 9 sample points were used to generate the original Kriging model, and the 9 sample points together with gradient information at these points were used for the Cokriging models. From the comparisons in Figure 1, it is clear that Cokriging models performed much better than the Kriging model in predicting the objective function for both its general shape and magnitude. The discrepancies of the original Kriging model were caused by under-sampling.

Very little difference was found between the direct and indirect Cokriging methods at least in this test case and therefore, we feel comfortable that we can use either of the two Cokriging approaches with similar accuracy. The indirect Cokriging method has the advantage of having a simpler formulation, but there is a chance for numerical errors to be introduced while estimating the additional function values from the gradients. The direct method can be more accurate because it uses gradient information directly, but the formulation becomes more complex as the dimensionality of the problem increases.

In order to investigate the applicability of the Cokriging models in 2-dimensional design spaces, C_D optimizations were performed using each of the approximation models generated above. Figure 2 (a) shows the C_D optimization results using the database constructed from 400 CFD calculations over the design space. The optimization was repeated five different times by changing the starting points. Four of them converged to one local minimum point and one converged to a different one. The optimizations were again repeated using different approximation models generated from Kriging and Cokriging methods, and the results are compared in the subsequent figures. As shown, the predicted optimum design point and optimum value of C_D for these cases were nearly identical. The predicted C_D from the CFD database was 0.0059708 whereas those for the Cokriging models with 5 and 9 sample points (and gradients) were 0.0059759 and 0.0059758 respectively with almost the same optimum design point locations. The relative error for the optimized C_D value is within 0.086%. As we can observe from Figure 2 (b), the ability of the original Kriging method to simulate the unknown function was clearly limited without an extensive set of sampled data. The optimum point and the predicted C_D value were far off from the actual ones.

5.2 Two-Dimensional Optimization Problem

C_D Optimization using Cokriging Model

The procedure used in the validation test case was repeated for this two-dimensional design problem with a different set of design variables. This time, the design variables and their range of variation were specifically selected to present a challenging boom minimization case. The two design variables selected represent the radii of two fuselage sections located at 10% and 20% of the length of the fuselage. A total of 121 CFD calculations were carried out and the results of the C_D variation over the design space are shown in Figure 3 (a). Even for this relatively simple function, the original Kriging model with 5 samples performed poorly in approximating the CFD calculations, whereas the two Cokriging approaches augmented by gradient information at the sample points were more successful in approximating the function. As in the test case, the C_D optimizations using Cokriging models were much more accurate than that using the original Kriging model in terms of both the ability to find the local minimum and to estimate the actual function values. Figure 4 shows the graphical representation of the optimization results.

Ground Boom Optimization using Cokriging Model

The general shape of the ground boom overpressure across the design space computed using the same 121 CFD calculations is shown in Figure 5 (a). Unlike the C_D objective function case, the values of the initial shock jump at the ground varies almost linearly with each design variable until sharp discontinuities are found for lower values of both design variables. This kind of functional variation is considered to be quite difficult to capture with a small number of sample data points. Subsequent Figures show the approximations of the exact boom overpressure values using both Kriging and Cokriging models with 5 sample data points.

Similarly to the previous test case, the accuracy of the Kriging model was greatly improved by the addition of gradient information.

Even though Cokriging models had some difficulty to capture the exact variation of the overpressures over the entire design space, three successive design iterations using a trust region methodology produced quite satisfactory results. Figure 6 (a) shows the history of sample points computed for all three design iterations as well as the evolution of the optimum design point superimposed on the exact CFD contour plot (for reference purposes only). Figures 6 (b),(c),(d) represent Cokriging models and the location of the sample points for each design iteration as well as the true and estimated optima for the Cokriging models. After three design iterations the actual location and the function value of the local minimum was achieved fairly accurately.

Figure 7 shows the result of a test case in which the effect of accumulating sample points was examined. As can be seen in Figure 7 (a), accumulating the 1^{st} and 2^{nd} sample sets greatly improved the ability of the Cokriging model to capture the general features of the target function over the complete design space. However, combining the 2^{nd} and 3^{rd} sets did not help the accuracy of the Cokriging model much. This is a consequence of the fact that a sharp discontinuity existed around the region of interest and the Cokriging model could not find accurate correlation parameters between all sample points. By retaining the sample points from the 1^{st} set, global information is used to model the discontinuity more accurately. These results are also repeated for the case of accumulating all three sample sets, which are shown in Figure 7 (d).

5.3 15-Dimensional Design Case

The last test case corresponds to the demonstration of the Cokriging method in a high-dimensional problem. In all the results that follow, the 15-dimensional parameterization of Section 3.3 will be used. The objective is to minimize a weighted combination of the drag coefficient, C_D, and the ground boom overpressure, Δp,

$$I = \alpha C_D + \beta \Delta p, \tag{16}$$

by varying the values of 15 configuration design variables. The only constraints imposed on the problem are upper and lower bounds on the design variables.

At each design iteration, Cokriging approximations of the C_D and Δp are constructed by running QSP107 at 31 sample points distributed in a *star* design. The *star* design consists of a central point and variations $\pm\Delta x_i$ along each of the design variables. In the first iteration of the procedure, the Δx_i values were chosen so that they had relatively high magnitude and the sampling spanned a large design space. For example, for the sweep angle of the wing, $\Delta x_i = \pm 10^\circ$. In subsequent iterations, Δx_i were monotonically decreased according to the bounds of the corresponding trust region.

Additional CFD computations using QSP107 were carried out to obtain the necessary finite-difference gradient information. This requirement resulted in a total of 496 CFD and boom propagation solutions. It must be mentioned that this approach was simply followed to accomplish our goals in a straightforward fashion. The proper way of obtaining gradient information would be by using the adjoint solver for QSP107. This would have resulted, instead, in an additional 31 CFD solutions, for a total of 62 solutions. This is quite a small number compared with the 496 actually used. As the number of design variables increases, the trade-off is even more compelling.

Figure 9 details the geometric meaning of all 15 design variables. Table 1 summarizes the results of all optimizations that were carried out. Although the primary results are those of the last row (C_D + Boom Optimization), we also conducted optimizations based on the C_D and boom overpressure alone for comparison purposes. The baseline design drag coefficient was found to be $C_D = 0.0088$ and the overpressure, $\Delta p = 0.77569$ psf.

C_D + Boom Optimization

In the last row of Table 1 we can see the results of three major iterations of the design procedure. At each iteration, a Cokriging approximation was constructed and a search for the global optimum was conducted by multiple runs of the *fmincon* algorithm. Once the global optimum had been found, a single CFD computation was carried out to identify the error in between the approximated and actual results. At that point, the trust region size was adjusted, and the procedure was repeated for a new Cokriging approximation centered about the location of the optimum of the previous iteration. The values for the weights were selected to be $\alpha = 50$, and $\beta = 1$.

In three design iterations, the C_D has decreased by 37.43%, while the boom has been attenuated by 18.57%. Since the design is not properly constrained, these numbers do not carry much meaning other than the fact that the optimization is lowering the value of the composite objective function. What is more relevant is the fact that the Cokriging approximation, at each design iteration is able to approximate both the C_D and Δp with relative errors that are always less than 5%. As the size of the trust region decreases, so do the errors, although not monotonically.

Figure 10 shows several views of the initial and optimized configurations. The main cause of the reduction of both the drag and the overpressures can be seen to be the increase in wing sweep to a rather large amount. This increase in sweep has the effect of spreading the lift over a longer distance which has beneficial effects for both sonic boom and performance. In addition, al-

though not clearly visible from the Figure, the fuselage area distribution has been tailored at all 5 design locations, the sweep of the canard has increased slightly. It must be noted that, although the wing sweep and location are rather extreme, they are not against the bounds of the design space. Finally, notice that the front portion of the fuselage has changed in shape significantly: the included angle at the nose decreases to weaken the leading shock, while a *bump* is formed right behind that causes a smooth recompression, followed by an expansion to weaken the overall effect on the overpressure.

Figure 11 shows both the near-field and ground pressure signatures for the original and optimized designs. It is found that the modifications to the fuselage shape, together with the location of the canard and the wing position and sweep cooperate to decrease the intensity of the initial shock and to prevent the coalescence of the wing leading edge shock.

C_D Optimization and Δp Optimization

The procedure followed for this C_D optimization is identical to that described previously, but the weight on Δp is $\beta = 0$. The results in the Table show the evolution of the design to the minimum at the third design iteration.

The results for the boom optimization are fairly similar. The ground overpressure decreases monotonically this time from an initial value of 0.77569 psf to 0.63858 psf. The geometries corresponding to both optimized results are relatively similar, with the wing sweep being again the dominant configuration variable.

It must be noted that in all three optimizations, the main stumbling block in the development of accurate Cokriging approximations is still the calculation of $\boldsymbol{\theta}$. This is particularly the case in the Indirect Cokriging method because, as the sample points get closer to each other, the correlation matrix may become ill-conditioned. Further research is needed to devise more robust methods for the computation of this parameter.

6. Conclusions

This paper explores the use of Cokriging approximate models for cost functions with multiple local minima and discontinuities in multi-dimensional space. If gradient information is available inexpensively, the Cokriging method is found to be superior to the original Kriging method for representation of complicated cost functions. Cokriging models depend heavily on the choice of the parameter $\boldsymbol{\theta}$, which normally results from an unconstrained optimization problem. More appropriate alternatives to the choice of $\boldsymbol{\theta}$ need to be investigated. Results are presented for sample two-dimensional test cases in order to visually validate the approximation functions. It is shown that reuse of information in the Cokriging approximation may both be beneficial and detrimental. Finally, design optimization based on a 15-dimensional academic test case is performed in order to minimize a weighted combination of the C_D and the ground boom overpressures.

7. Acknowledgments

The authors wish to acknowledge the support of the Defense Advanced Research Projects Agency QSP program under grant number MDA972-01-2-0003.

References

[1]Thomas A. Zang and Lawrence L. Green. "Multidisciplinary Design Optimization Technique: Implications and Opportunities for Fluid Dynamics" *30th AIAA Fluid Dynamics Conference*, Norfolk, Virginia, AIAA 99-3798, June 1999

[2]Jaroslaw Sobieszczanski-Sobieski and Raphael T. Haftka "Multidisciplinary Aerospace Design Optimization: Survey of Recent Developments," *34th AIAA Aerospace Sciences Meeting and Exhibit* , Reno, Nevada, AIAA 96-0711, January 1996.

[3]J. Martin, J. J. Alonso and J. Reuther "High-Fidelity Aero-Structural Design Optimization of a Supersonic Business Jet," *43rd AIAA/ASME/ASCE/AHS/ASC Structures, Structural Dynamics, and Materials Conference*, AIAA 2002-1483, Denver, CO, April 2002.

[4]J. Martin and J. J. Alonso "Complete Configuration Aero-Structural Optimization Using a Coupled Sensitivity Analysis Method," *9th AIAA/ISSMO Symposium on Multidisciplinary Analysis and Optimization*, AIAA 2002-5402 Atlanta, GA, September 2002.

[5]Resit Unal, Roger A. Lepsch, Jr. and Mark L. McMillin "Response Surface Model Building and Multidisciplinary Optimization Using Overdetermined D-Optimal Designs," *7th AIAA/USAF/NASA/ISSMO Symposium on Multidisciplinary Analysis and Optimization*, AIAA 98-4759, September 1998

[6]Anthony A. Giunta and Layne T. Watson "A Comparison of Approximation Modeling Techniques: Polynomial Versus Interpolating Models," *7th AIAA/USAF/NASA/ISSMO Symposium on Multidisciplinary Analysis and Optimization* , St. Louis, Missouri, AIAA 98-4758, September 1998.

[7]J. Sacks, W. J. Welch, T. J. Michell, and H. P. Wynn "Design and Analysis of Computer Experiments," *Statistical Science Vol 4. No.4*, pp. 409-453, 1989

[8]Timothy W. Simpson, Timothy M. Mauery, John J. Korte and Farrokh Mistree "Comparison of Response Surface and Kriging Models in the Multidisciplinary Design of an Aerospike Nozzle," *7th AIAA/USAF/NASA/ISSMO Symposium on Multidisciplinary Analysis and Optimization*, St. Louis, Missouri, AIAA 98-4755, September 1998

[9]H. Chung and J. J. Alonso "Using Gradients to Construct Cokriging Approximation Models for High-Dimensional Design Optimization Problems," *40th AIAA Aerospace Sciences Meeting and Exhibit*, AIAA 2002-0317, Reno, NV, January 2002.

[10]W. Liu and S. Batill "Gradient-Enhanced Response Surface Approximations Using Kriging Models," *9th AIAA/ISSMO Symposium on Multidisciplinary Analysis and Optimization*, AIAA 2002-5456, Atlanta, GA, September 2002.

[11]J. R. Koehler and A. B. Owen "Computer Experiments," *Handbook of Statistics Vol. 13*, pp. 261-308, Elsevier Science, New York, eds. S. Ghosh and C. R. Rao

[12]Edward H. Isaaks and R. Mohan Srivastava *An Introduction to Applied Geostatistics*, Oxford Univ. Press, Oxford, 1989.

[13]James J. Reuther, Antony Jameson, and Juan J. Alonso "Constrained Multipoint Aerodynamic Shape Optimization Using an Adjoint Formulation and Parallel Computers, Parts I and II," *Journal of Aircraft* Vol 36, No 1, January-February, 1999

[14]A. Jameson and T.J. Baker "Multigrid Solution of the Euler Equations for Aircraft Configurations," *AIAA Paper 84-0093*, Jan. 1984.

[15]A. Jameson, W. Schmidt, and E. Turkel "Numerical Solutions of the Euler Equations by Finite Volume Methods with Runge-Kutta Time Stepping Schemes," *AIAA Paper 81-1259*, Jan. 1981.

[16]A. Jameson "Multigrid Algorithms for Compressible Flow Calculations," *Lecture Note in Mathematics* edited by W. Hackbusch and V. Trottenberg, Vol. 1228, Springer-Verlag, 1986.

[17]A. Jameson "Optimum Aerodynamic Design Using CFD and Control Theory" *AIAA 12th Computational Fluid Dynamics Conference* , AIAA paper 95-1729, San Diego, CA, 1995.

[18]A. Jameson, L. Martinelli and N. A. Pierce "Optimum Aerodynamic Design Using the Navier-Stokes Equations," *Theoretical and Computational Fluid Dynamics* Vol 10, pp. 231–237, 1998.

[19]A. Jameson, N. Pierce and L. Martinelli "Optimum Aerodynamic Design Using the Navier-Stokes Equations," *AIAA Paper 97-0101*, Jan. 1997.

[20]Kenneth J. Plotkin "PCBoom3 Sonic Boom Prediction Model-Version 1.0e," *Wyle Research Report WR 95-22E*, October. 1998.

[21] *Optimization Toolbox For Use with MATLAB, Version 2*, The MathWorks, Inc. Mass., July, 2002

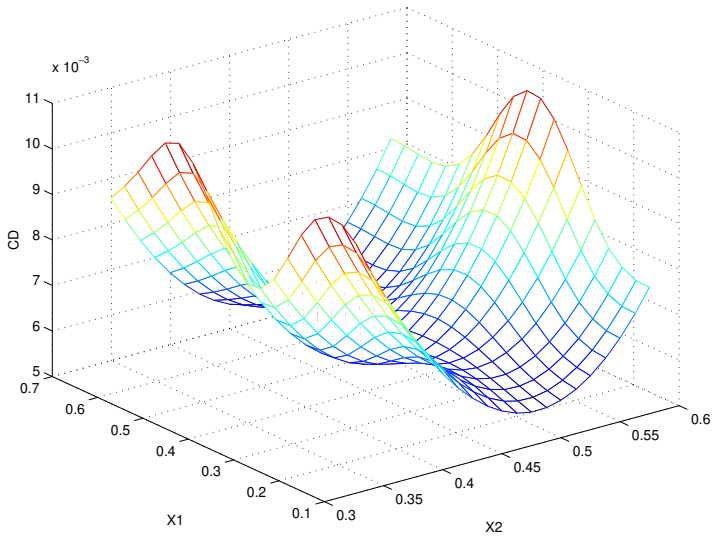

(a) Results of CFD Calculations over 400 Design Points

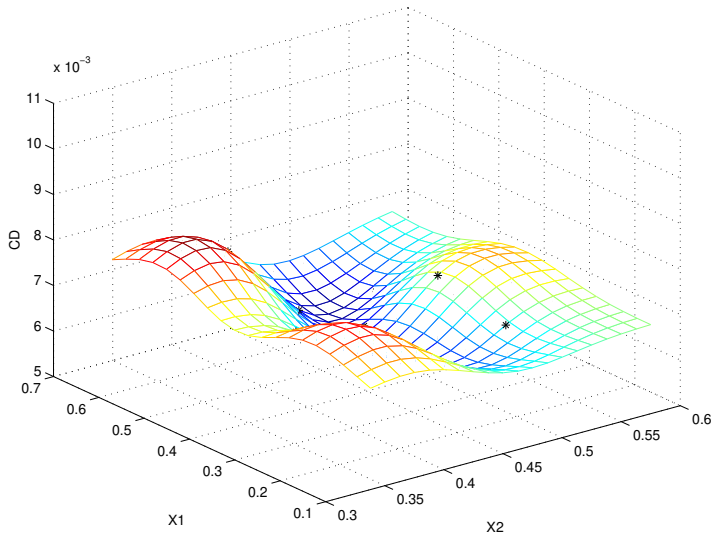

(b) Original Kriging Model with 9 Sample Values

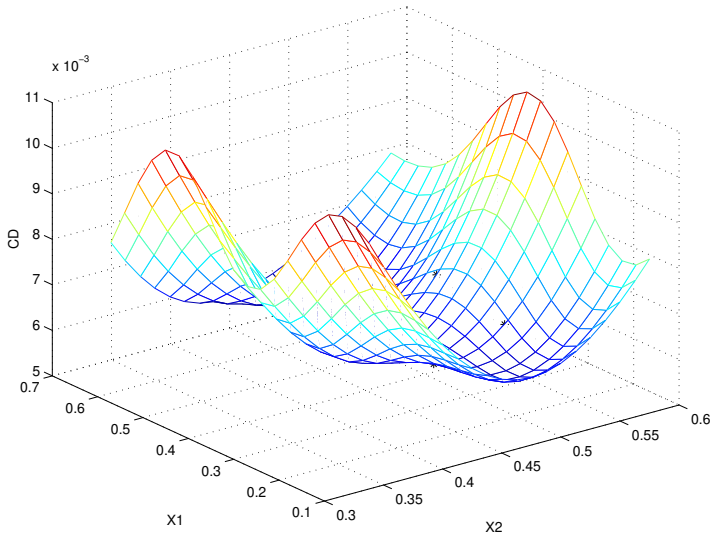

(c) Direct Cokriging Model with 9 Sample Values and their Gradients

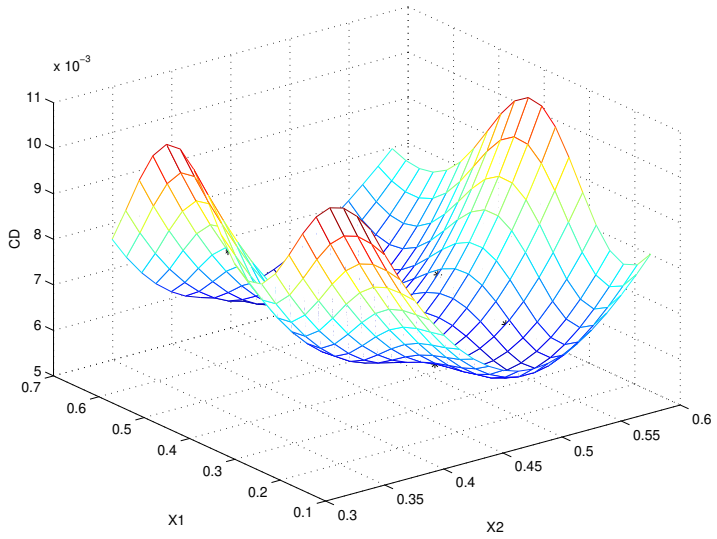

(d) Indirect Cokriging Model with 9 Samples and 18 Additional Values Obtained from Gradients

Fig. 1 Validation Problem. C_D Cokriging Models for 2-D SBJ Test Case Using Two Design Variables: Wing Position and Fuselage Radius at 50% Location

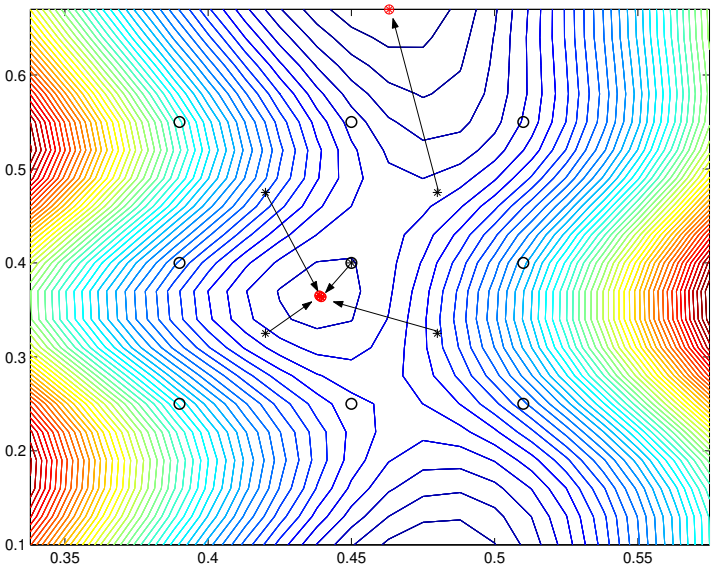

(a) C_D Optimization Using CFD Calculation Results over 400 Design Points

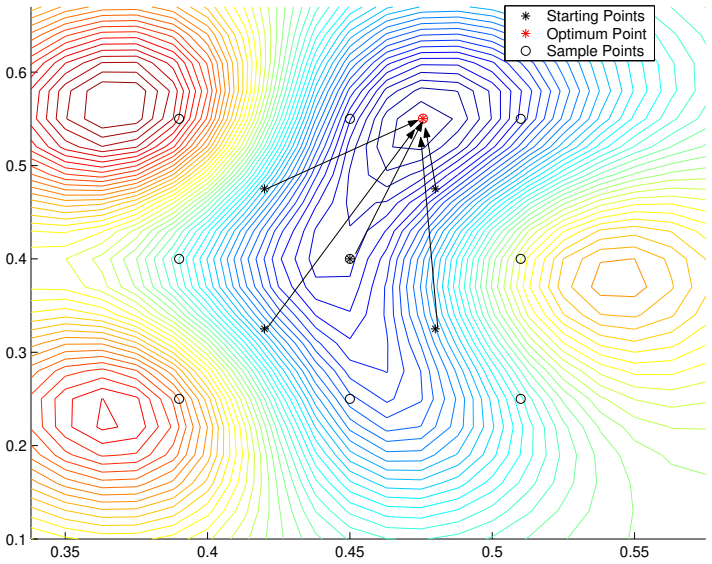

(b) C_D Optimization Using Original Kriging Model with 9 Sample Values

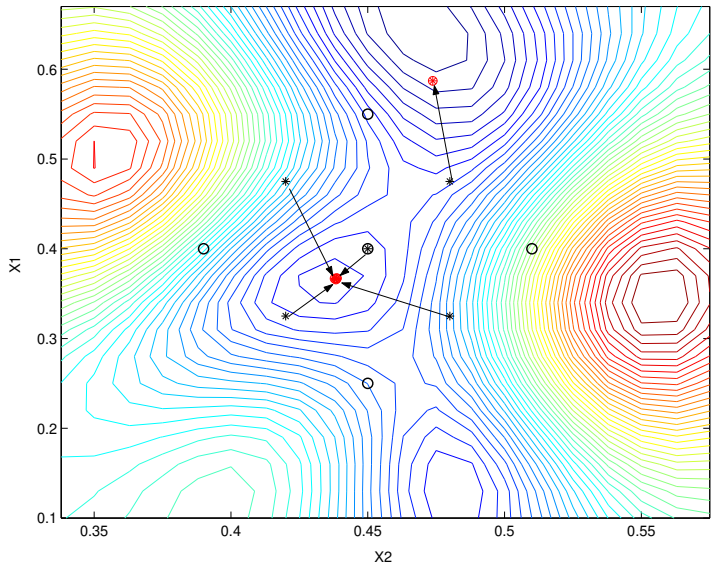

(c) C_D Optimization Using Cokriging Model with 5 Sample Values and their Gradients

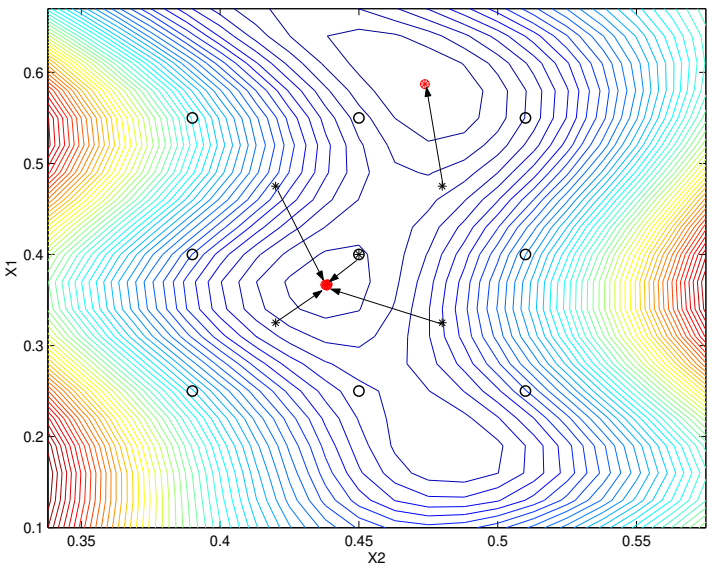

(d) C_D Optimization Using Cokriging Model with 9 Sample Values and their Gradients

Fig. 2 C_D **Optimization Results for 2-D SBJ Test Case**

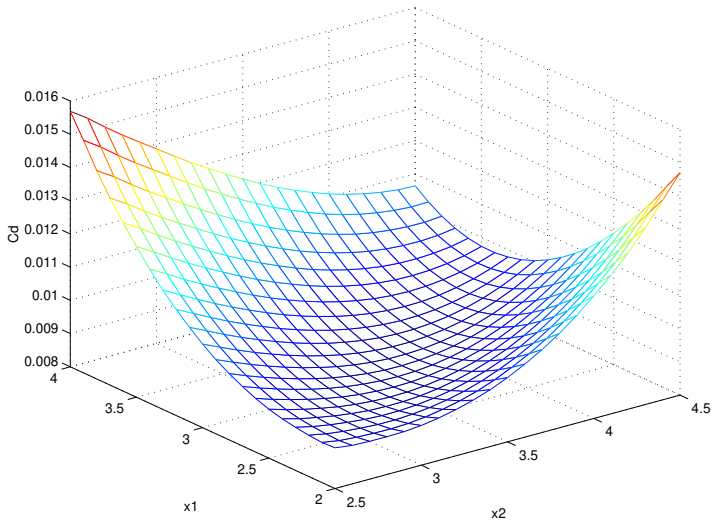

(a) Results of CFD Calculations over 121 Design Points

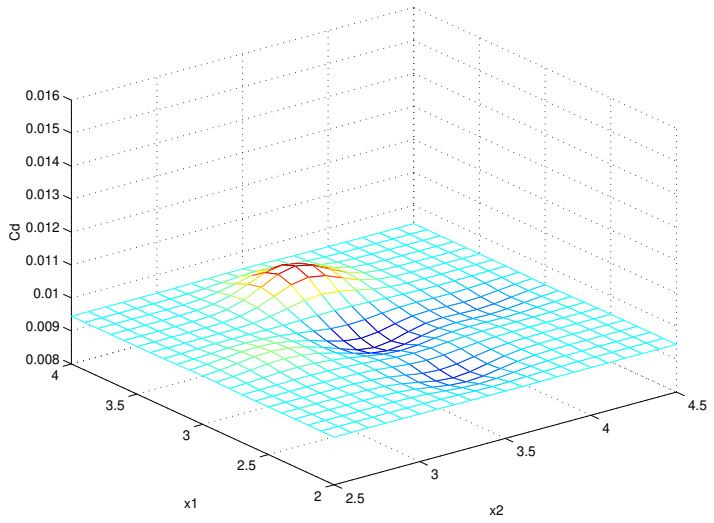

(b) Original Kriging Model with 5 Sample Values

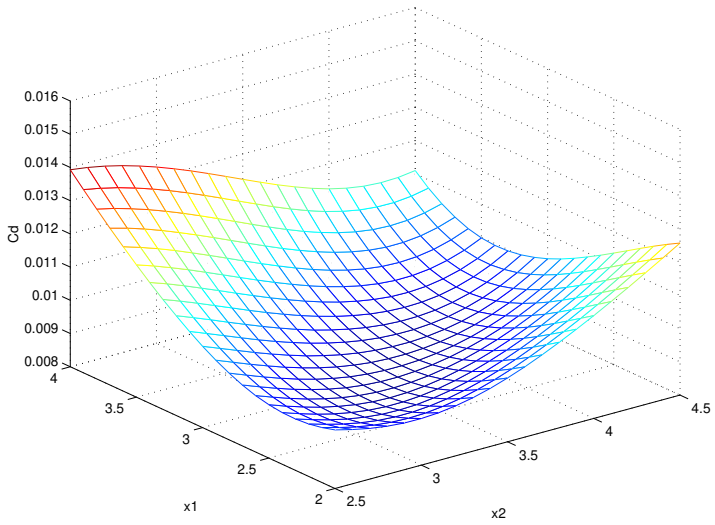

(c) Direct Cokriging Model with 5 Sample Values and their Gradients

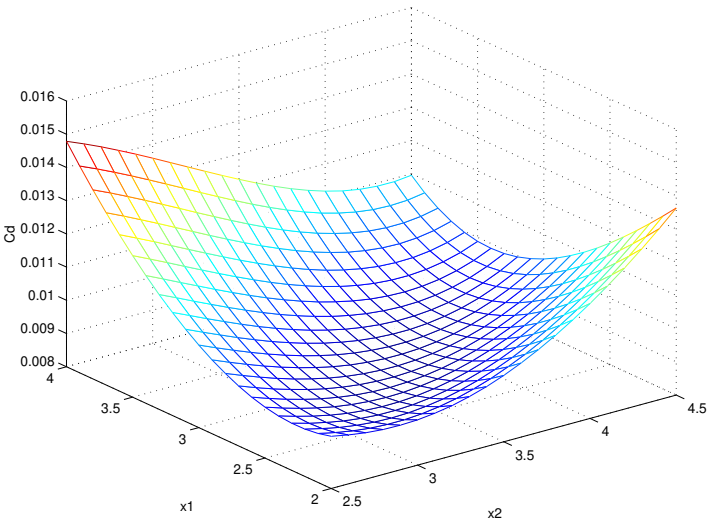

(d) Indirect Cokriging Model with 5 Samples and 10 Additional Values Obtained from Gradients

Fig. 3 C_D Cokriging Models for 2-D SBJ Design Problem Using Two Design Variables: Fuselage Radii at 10% and 20% Locations

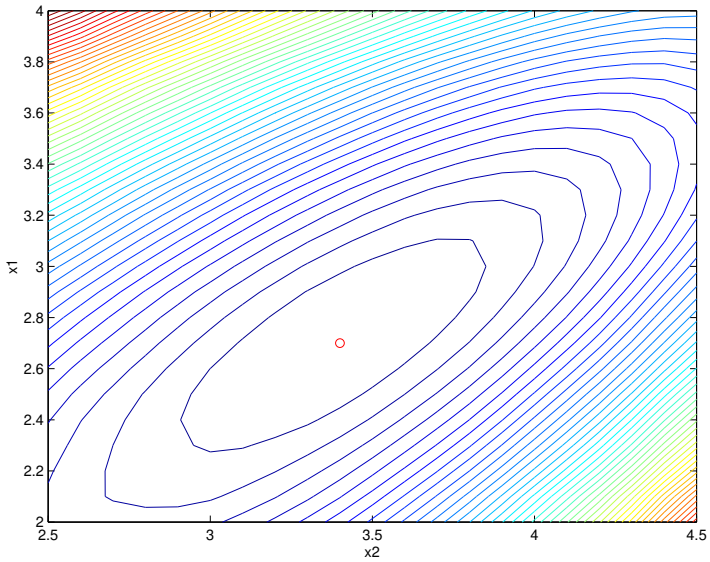

(a) Results of CFD Calculations over 121 Design Points

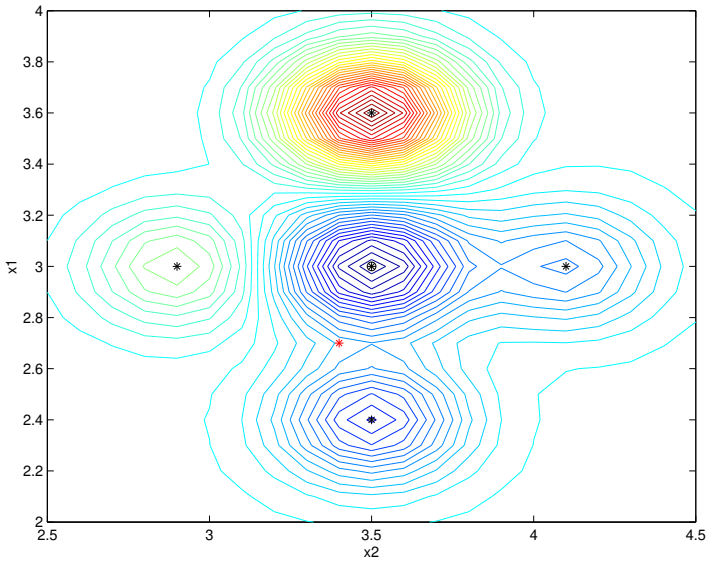

(b) Original Kriging Model with 5 Sample Values

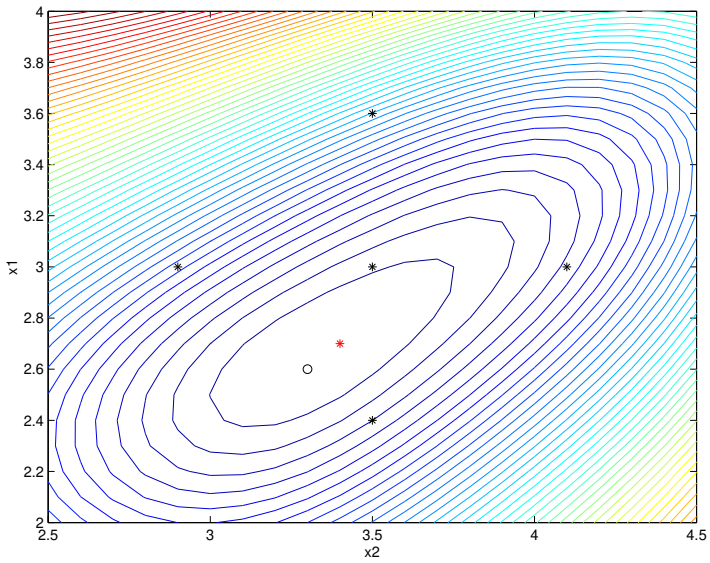

(c) Direct Cokriging Model with 5 Sample Values and their Gradients

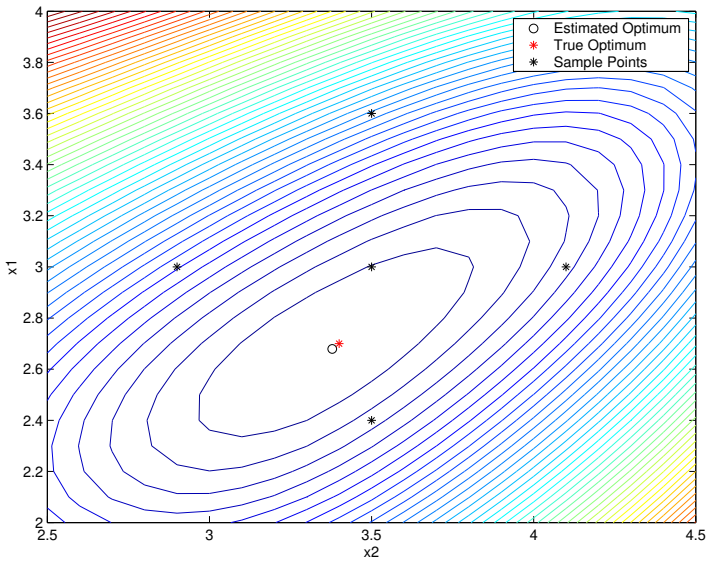

(d) Indirect Cokriging Model with 5 Samples and 10 additional Values Obtained from Gradients

Fig. 4 C_D Optimization Results for 2-D SBJ Design Problem

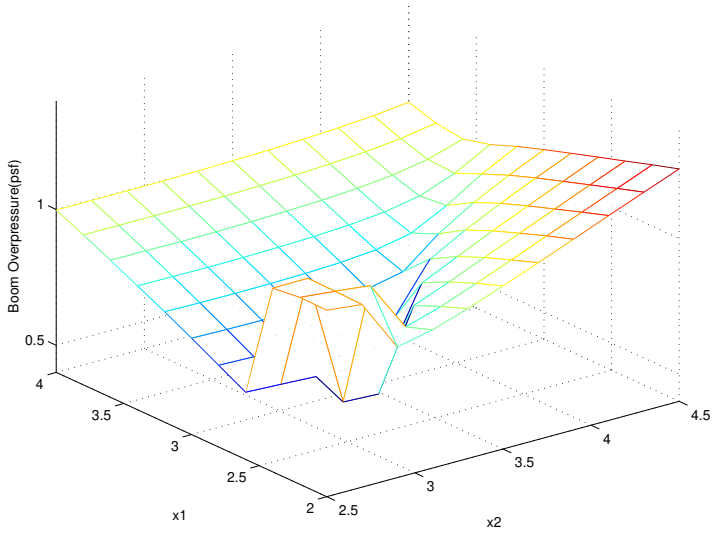

(a) Results of CFD Calculations over 121 Design Points

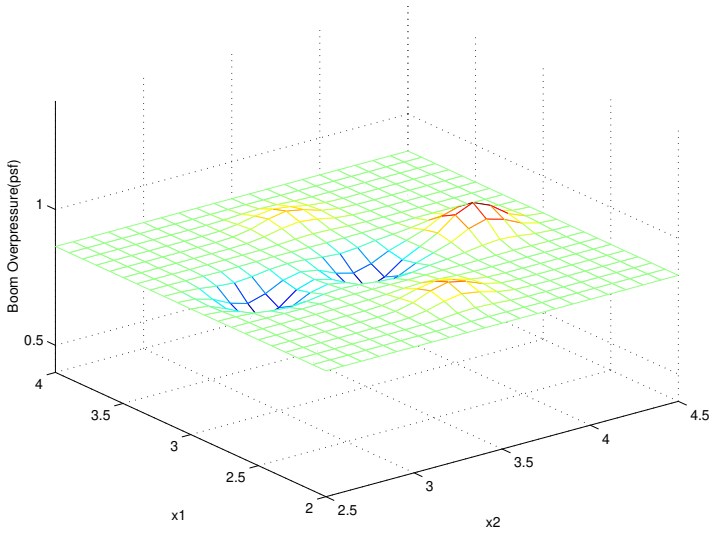

(b) Original Kriging Model with 5 Sample Values

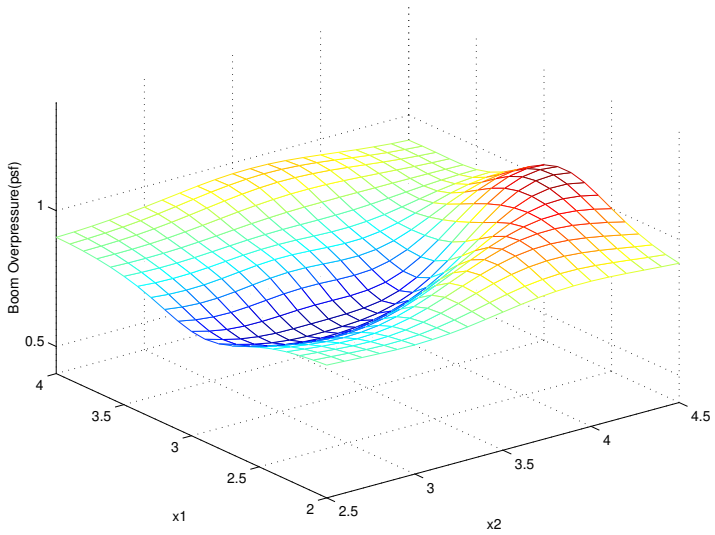

(c) Cokriging Model with 5 Sample Values and their Gradients

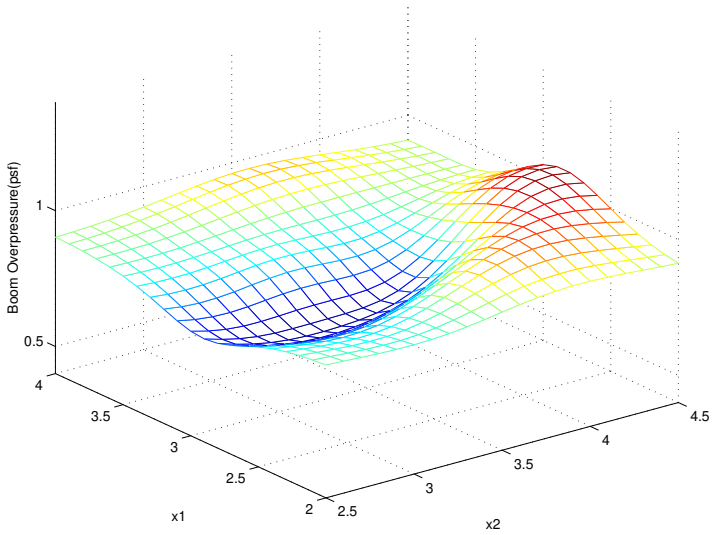

(d) Cokriging Model with 5 Samples and 10 Additional Values Obtained from Gradients

Fig. 5 Boom Overpressure Cokriging Models for 2-D SBJ Design Problem Using Two Design Variables: Fuselage Radii at 10% and 20% Locations

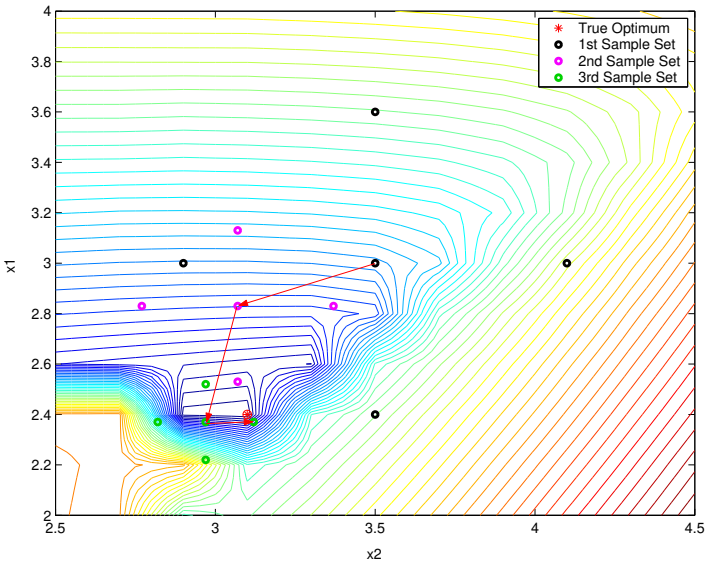

(a) Sample Points Over 3 Design Iterations and Optimum Design Evolution With Contours from CFD Calculations

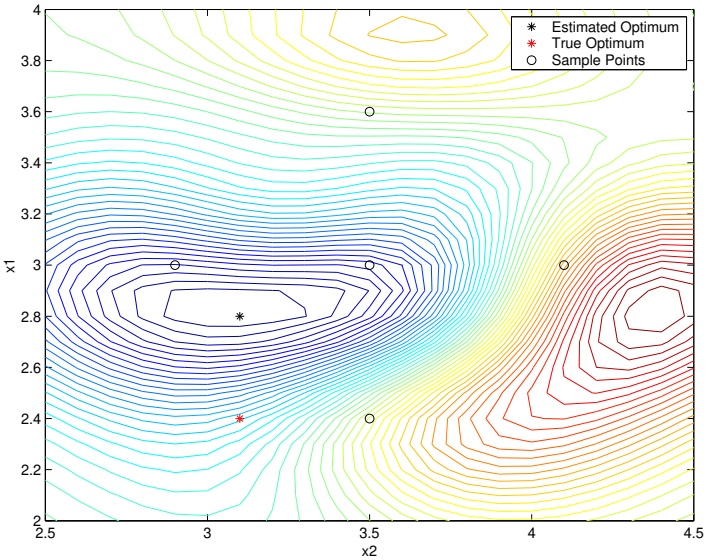

(b) 1^{st} Design Cycle Results with Cokriging Approximation Contour Plot

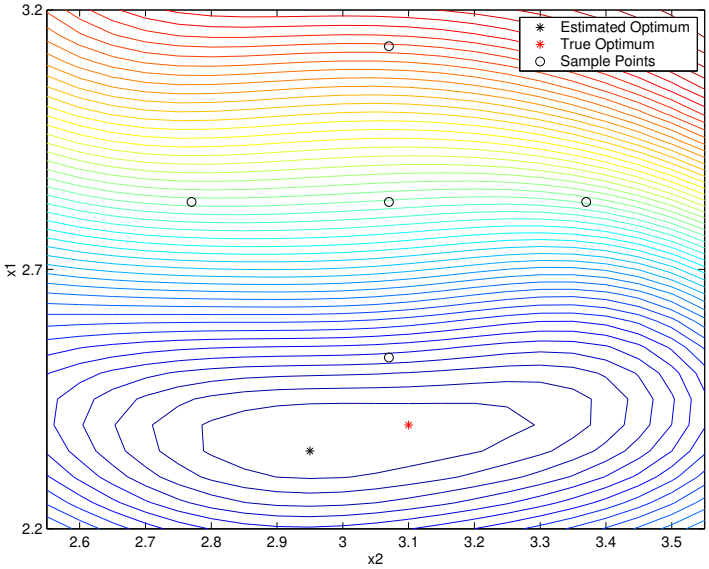

(c) 2^{nd} Design Cycle Results with Cokriging Approximation Contour Plot

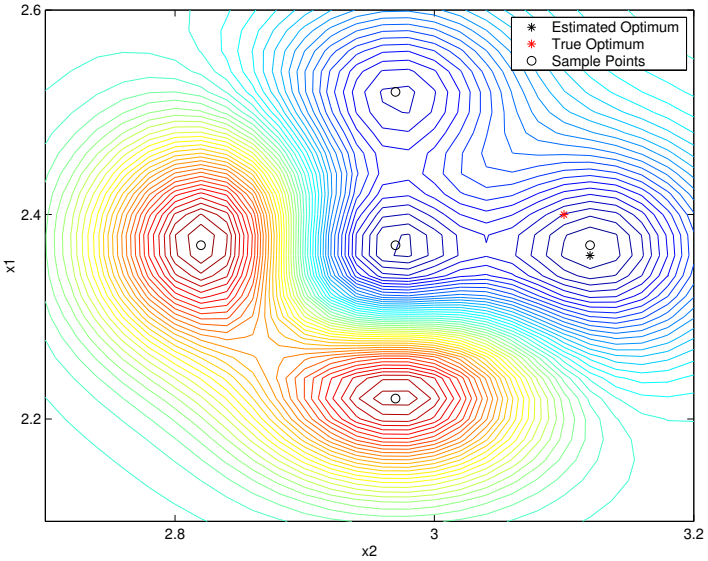

(d) 3^{rd} Design Cycle Results with Cokriging Approximation Contour Plot

Fig. 6 Boom Overpressure Optimization Results using Indirect Cokriging Method for 2-D SBJ Design Problem

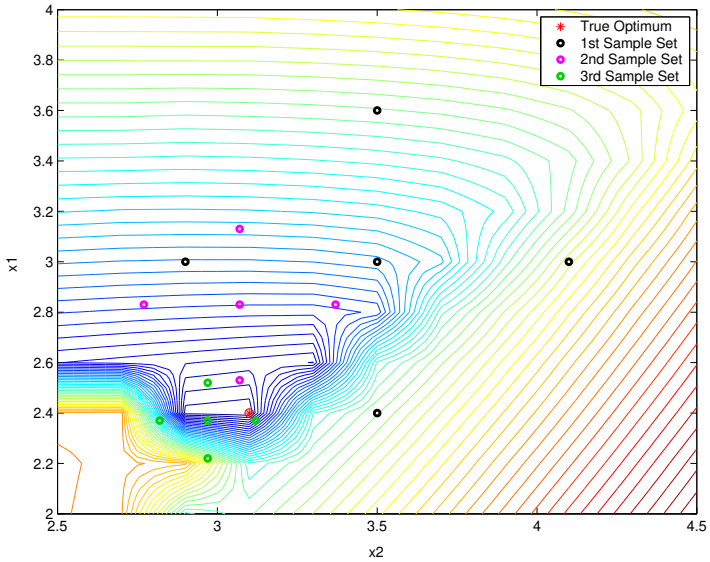

(a) Results of CFD Calculations over 121 Design Points with Sample Data Locations

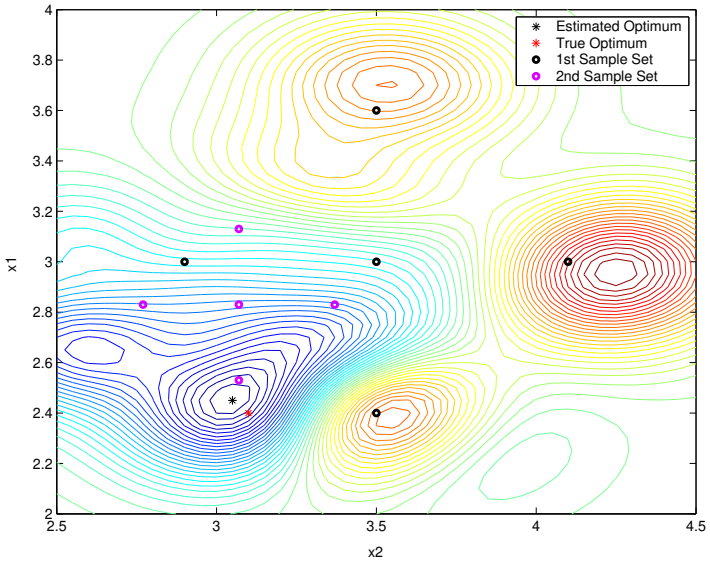

(b) Cokriging Approximation using First and Second Sample Sets

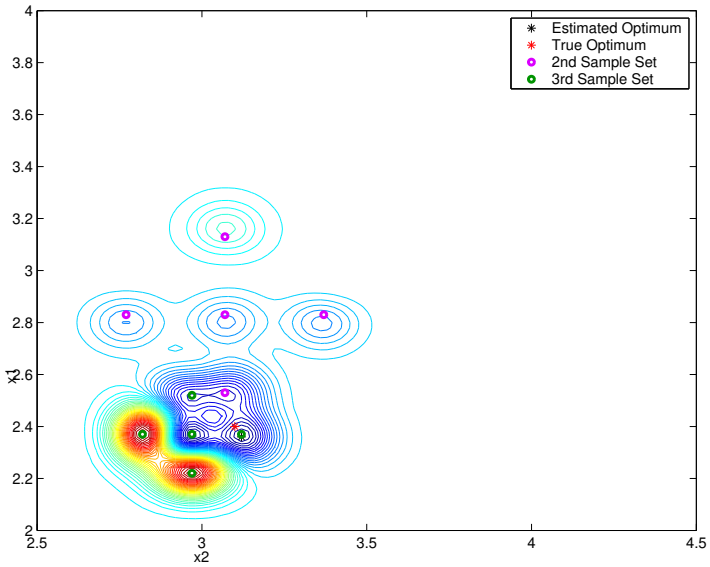

(c) Cokriging Approximation Using Second and Third Sample Sets

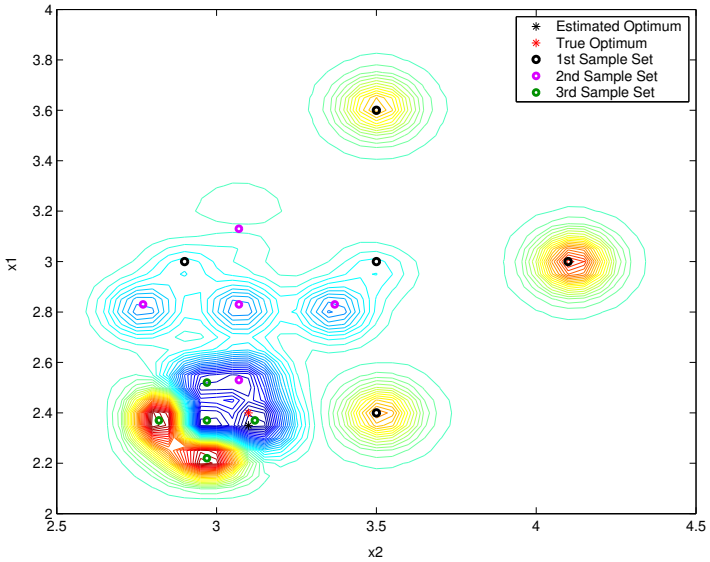

(d) Cokriging Approximation using First, Second, and Third Sample Sets

Fig. 7 Boom Overpressure Contour Plots of Indirect Cokriging Models for 2-D SBJ Design Problem Using Different Amount and Locations of Sample Values

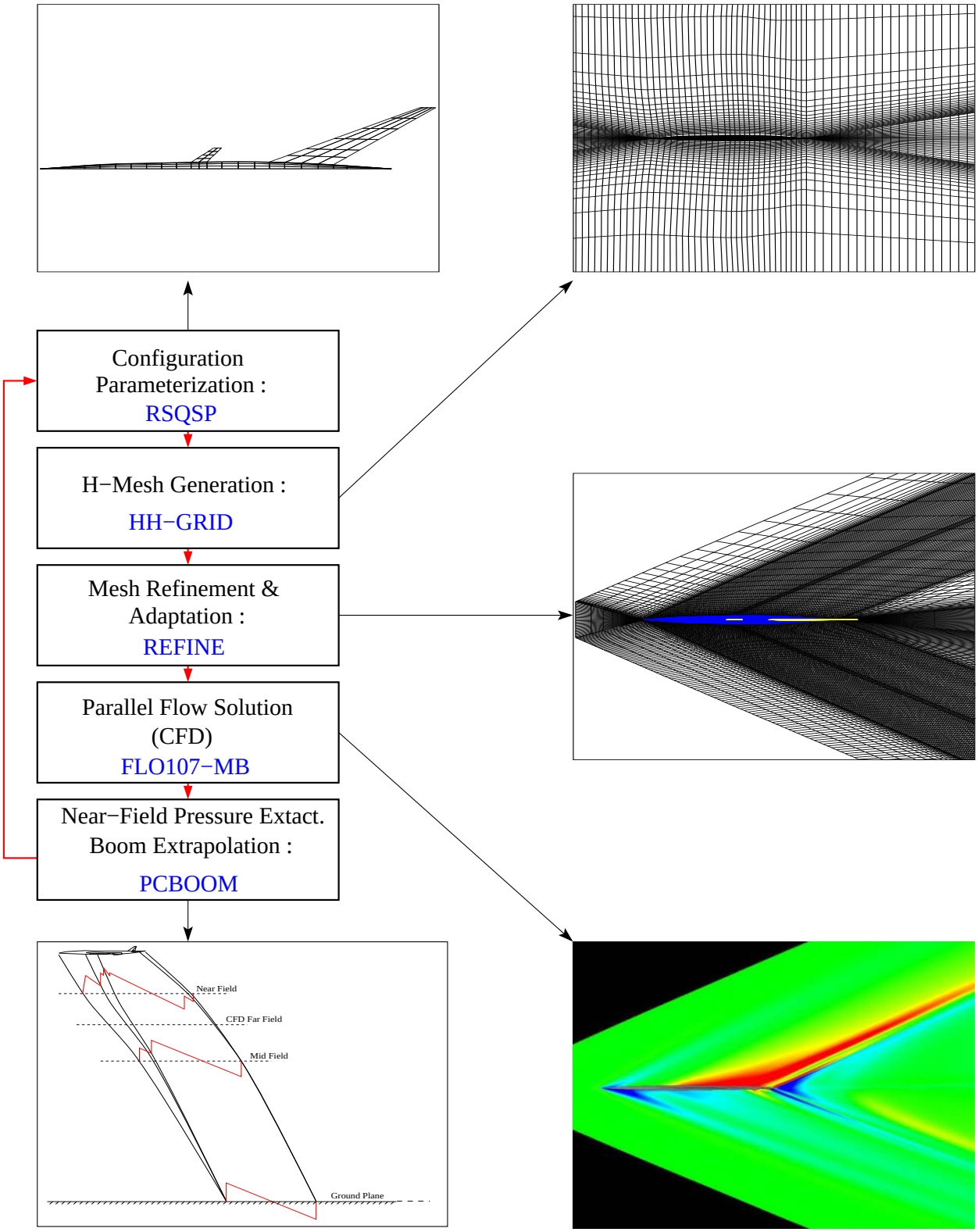

Fig. 8 Flowchart of the Various Modules of QSP107 Design Tool

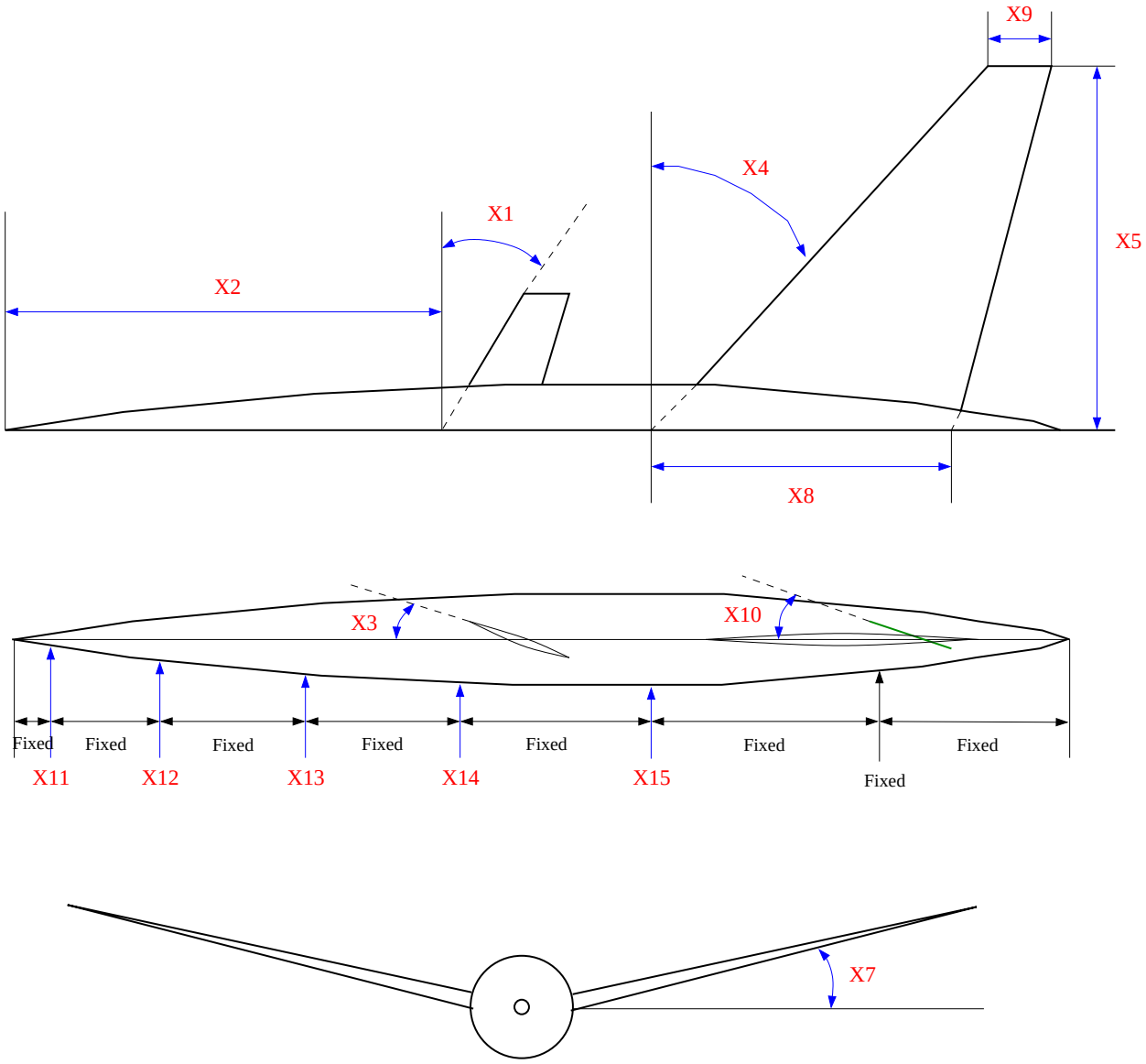

Design Variables

Canard	Wing	Fuselage
X1 : Canard Sweep Angle	X4 : Wing Sweep Angle	X11 : Fuselage Radius at 3% Fuselage Length
X2 : Canard X−Position	X5 : Wing Aspect Ratio	X12 : Fuselage Radius at 10% Fuselage Length
X3 : Canard Twist Angle	X6 : Wing Taper Ratio	X13 : Fuselage Radius at 20% Fuselage Length
	X7 : Wing Dihedral Angle	X14 : Fuselage Radius at 30% Fuselage Length
	X8 : Wing Root TOC	X15 : Fuselage Radius at 55% Fuselage Length
	X9 : Wing Tip TOC	
	X10: Wing Tip Twist	

Fig. 9 Definition of Design Variables for 15-Dimensional SBJ Design Problem

		1^{st} Design Cycle	2^{nd} Design Cycle	3^{rd} Design Cycle
C_D Optimization	Optimum Design	$x_1 = 44.30$ $x_2 = 0.400$ x_3 =-0.216 $x_4 = 70.64$ $x_5 = 4.034$ $x_6 = 0.200$ x_7 =-0.013 $x_8 = 3.906$ $x_9 = 3.928$ x_{10}=-1.201 x_{11}= 0.459 x_{12}= 1.684 x_{13}= 2.941 x_{14}= 3.493 x_{15}= 4.458	$x_1 = 45.94$ $x_2 = 0.410$ x_3 =-0.460 $x_4 = 70.10$ $x_5 = 4.514$ $x_6 = 0.227$ $x_7 = 0.182$ $x_8 = 3.574$ $x_9 = 3.744$ x_{10}=-1.454 x_{11}= 0.523 x_{12}= 1.694 x_{13}= 2.837 x_{14}= 3.517 x_{15}= 4.422	$x_1 = 45.05$ $x_2 = 0.395$ x_3 =-0.217 $x_4 = 70.26$ $x_5 = 4.439$ $x_6 = 0.237$ $x_7 = 0.191$ $x_8 = 3.625$ $x_9 = 3.790$ x_{10}=-0.532 x_{11}= 0.478 x_{12}= 1.767 x_{13}= 2.809 x_{14}= 3.415 x_{15}= 4.329
	Predicted Optimum	0.0054456	0.0051252	0.0052336
	Verified Optimum*	**0.0053675**	**0.0049775**	**0.0051196**
	% Error	1.455	2.967	2.230
Sonic Boom Optimization	Optimum Design	$x_1 = 46.82$ $x_2 = 0.407$ $x_3 = 0.258$ $x_4 = 60.71$ $x_5 = 4.091$ $x_6 = 0.212$ $x_7 = 0.121$ $x_8 = 4.094$ $x_9 = 4.098$ x_{10}= 1.036 x_{11}= 0.452 x_{12}= 1.915 x_{13}= 2.952 x_{14}= 3.491 x_{15}= 4.592	$x_1 = 45.77$ $x_2 = 0.394$ $x_3 = 0.014$ $x_4 = 69.90$ $x_5 = 4.100$ $x_6 = 0.221$ $x_7 = 0.173$ $x_8 = 3.984$ $x_9 = 4.004$ x_{10}= 0.104 x_{11}= 0.426 x_{12}= 1.865 x_{13}= 2.848 x_{14}= 3.440 x_{15}= 4.664	$x_1 = 45.46$ $x_2 = 0.387$ x_3 =-0.023 $x_4 = 70.15$ $x_5 = 4.233$ $x_6 = 0.229$ $x_7 = 0.204$ $x_8 = 3.855$ $x_9 = 3.922$ x_{10}=-0.159 x_{11}= 0.441 x_{12}= 1.857 x_{13}= 2.684 x_{14}= 3.424 x_{15}= 4.395
	Predicted Optimum	0.70278	0.64847	0.62872
	Verified Optimum*	**0.69947**	**0.68337**	**0.63858**
	% Error	0.473	0.718	1.544
C_D + Boom Multi-Objective Optimization	Optimum Design	$x_1 = 45.92$ $x_2 = 0.404$ x_3 =-0.050 $x_4 = 70.00$ $x_5 = 4.068$ $x_6 = 0.207$ $x_7 = 0.016$ $x_8 = 3.952$ $x_9 = 3.954$ x_{10}=-1.094 x_{11}= 0.448 x_{12}= 1.814 x_{13}= 2.829 x_{14}= 3.487 x_{15}= 4.540	$x_1 = 45.04$ $x_2 = 0.393$ x_3 =-0.051 $x_4 = 70.14$ $x_5 = 4.226$ $x_6 = 0.228$ $x_7 = 0.151$ $x_8 = 3.844$ $x_9 = 3.914$ x_{10}=-0.193 x_{11}= 0.437 x_{12}= 1.840 x_{13}= 2.839 x_{14}= 3.418 x_{15}= 4.390	$x_1 = 45.50$ $x_2 = 0.387$ x_3 =-0.040 $x_4 = 70.33$ $x_5 = 4.235$ $x_6 = 0.230$ $x_7 = 0.204$ $x_8 = 3.838$ $x_9 = 3.915$ x_{10}=-0.182 x_{11}= 0.445 x_{12}= 1.844 x_{13}= 2.685 x_{14}= 3.422 x_{15}= 4.388
	Predicted Optimum	C_D = 0.0060186 Boom = 0.74181	C_D = 0.0056938 Boom = 0.68679	C_D = 0.0055236 Boom = 0.63164
	Verified Optimum*	C_D **= 0.0057324** **Boom = 0.71980**	C_D **= 0.0055761** **Boom = 0.68615**	C_D **= 0.0055115** **Boom = 0.63794**
	% Error	Error_C_D = 4.990 Error_Boom = 3.058	Error_C_D = 2.110 Error_Boom = 0.093	Error_C_D = 0.220 Error_Boom = 0.988

Table 1 Summary of Results for 15-Dimensional Optimization Case (* Calculated using CFD analysis code with predicted optimum design

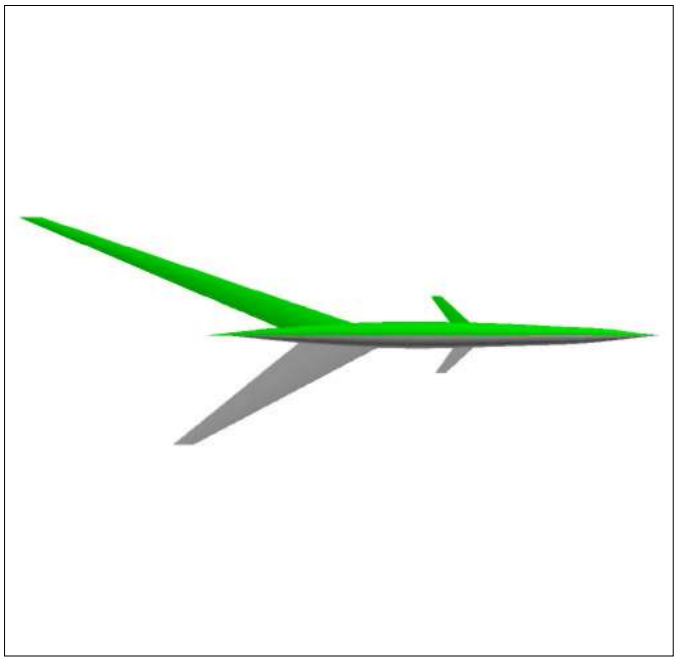

(a) Base(Grey) and Final Design(Green) Configuration Comparison : Top View

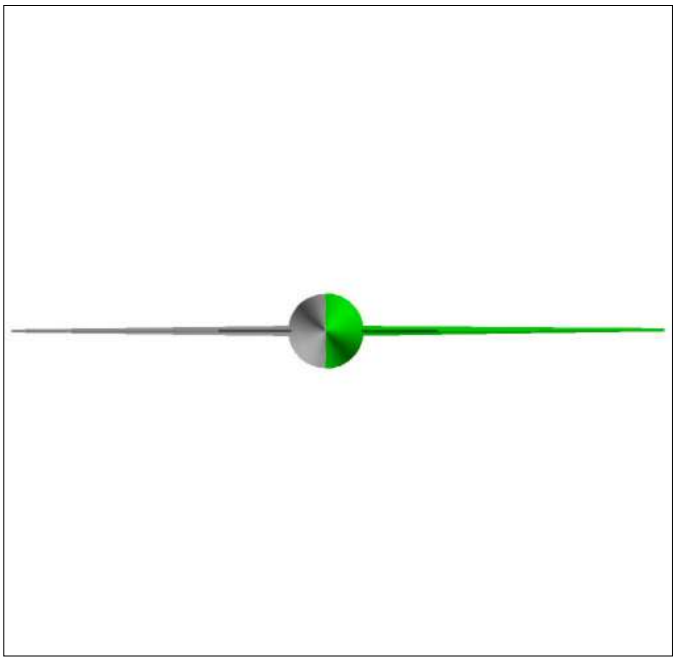

(b) Base(Grey) and Final Design(Green) Configuration Comparison : Front View

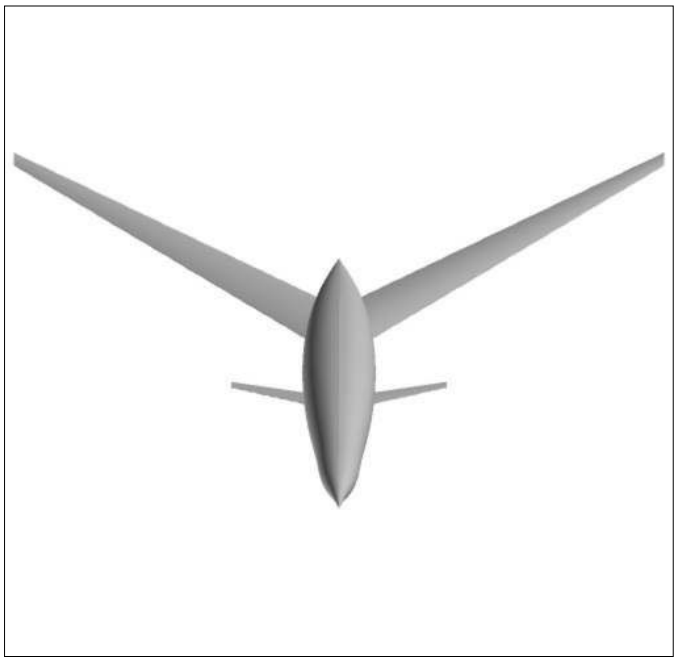

(c) Final Design Configuration

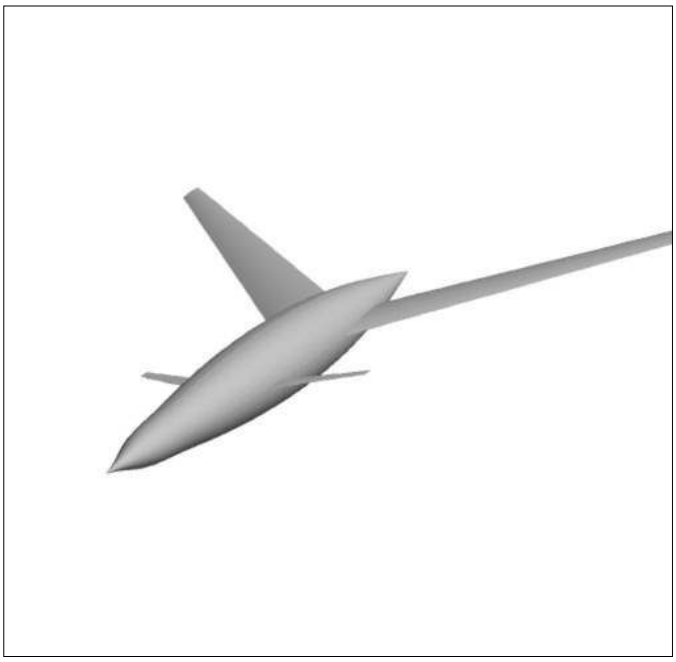

(d) Final Design Configuration

Fig. 10 Final Design Configuration Drawings

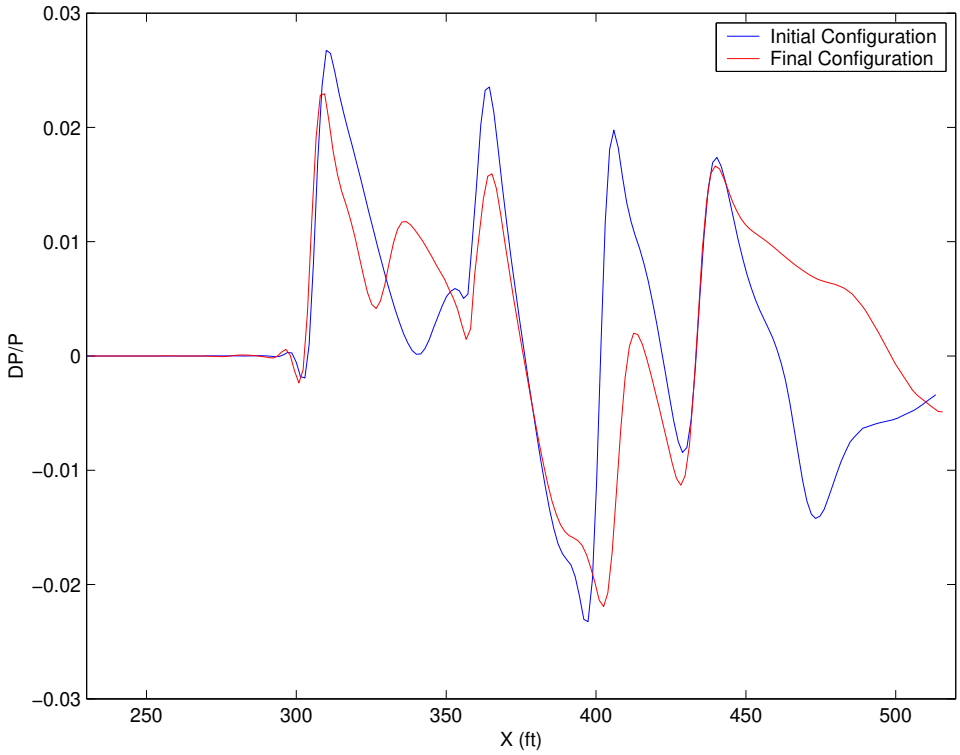

(a) Near-Field Pressure Distribution Comparison

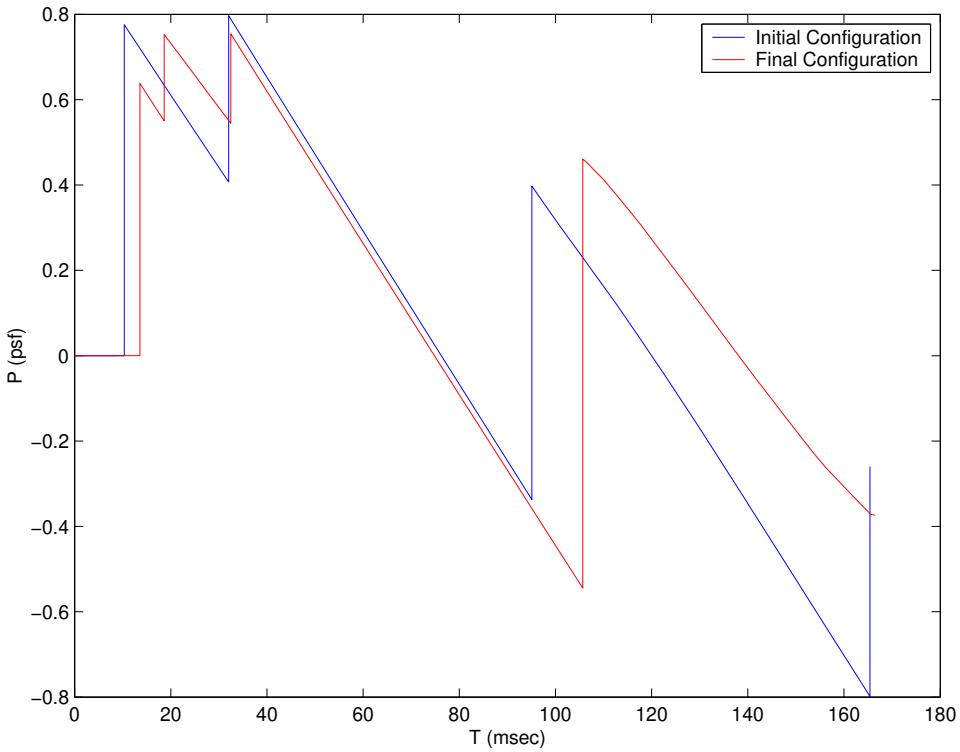

(b) Ground Boom Comparison

Fig. 11 Comparison Between Base and Final Design Configurations for 15-Dimensional SBJ Design Problem